We are IntechOpen, the world's leading publisher of Open Access books Built by scientists, for scientists

6,900
Open access books available

185,000
International authors and editors

200M
Downloads

Our authors are among the

154
Countries delivered to

TOP 1%
most cited scientists

12.2%
Contributors from top 500 universities



WEB OF SCIENCE™

Selection of our books indexed in the Book Citation Index in Web of Science™ Core Collection (BKCI)

Interested in publishing with us?
Contact book.department@intechopen.com

Numbers displayed above are based on latest data collected.
For more information visit www.intechopen.com



Chapter 4

Indirect Extrusion: A Multifaceted Approach of Sub-surface Tubular Expansion

Tasneem Pervez, Sayyad Z. Qamar,
Omar S.A. Al-Abri and Rashid Khan

Additional information is available at the end of the chapter

http://dx.doi.org/10.5772/intechopen.70311

Abstract

Extrusion and indirect extrusion is a very old manufacturing process used in multitudes of applications mainly focused on transportation, household and power industries. Indirect extrusion has found an interesting application in petroleum industry, which resulted in resolving many unsolvable issues over the last few decades. The current and expected future global demand for hydrocarbons became a driving force for researchers to find new comprehensive and cheaper solutions for hydrocarbon production. The challenges faced in oil and gas fields, while drilling, constructing and operating new and old vertical/horizontal wells, are many. The use of indirect extrusion for in-situ expansion of sub-surface tubulars used in wells revolutionized the drilling and completion as opposed to one and half decade back. The emergence of solid expandable tubular technology has changed the basics of how we design and construct wells. The original development of the technology was to overcome the challenges faced by the petroleum industry to reach ultra-deep reservoirs, off-shore drilling, drilling in high-pressure/difficult zones and repair/maintenance of old/ageing wells. However, it gained significant interest of researchers and operators in providing solutions to wide-range problems. The development of a computational framework using finite element method (FEM) enabled to determine the force required for expansion and resulting dimensional changes in final product, which is of direct assistance to the field engineers. The effect of friction and stress variations along contact surface is also determined.

Keywords: indirect extrusion, tubular expansion, oil and gas wells, finite element method, solid expandable tubular, nonlinear analysis

INTECH
open science | open minds

© 2018 The Author(s). Licensee InTech. This chapter is distributed under the terms of the Creative Commons Attribution License (http://creativecommons.org/licenses/by/3.0), which permits unrestricted use, distribution, and reproduction in any medium, provided the original work is properly cited. CC BY

1. Introduction

Extrusion is the process by which a block/billet of metal is reduced in cross section by forcing it to flow through a die orifice under high pressure. It is classified as: (a) Direct Extrusion, in which the ram of the machinery moves and forces the billet (semifinished metal form) through the die and (b) Indirect Extrusion, in which the ram is stationary and the die moves forcing the billet through the die. The process keeps the die stationary using a stem that is longer than the container containing the billet. Pipe extrusion is another process by which various forms of pipes are manufactured using a broad range of polymers selected based on intended usage. Pipes made of aluminum are also manufactured using extrusion. However, an interesting form of indirect extrusion occurs, when ferrous metal pipes are *in situ* expanded by forcing the die to pass through it. This novel use of pipe manufacturing, when extended for subsurface applications results in expanded pipe and is termed as solid expandable tubular (SET). The use of solid expandable tubular has made huge strides in the way the oil and gas wells are drilled and completed. Not only this, it has proven that the technique is able to provide solution to many unresolved problems faced by the petroleum industry.

Solid expandable tubular technology is a recent development in petroleum exploration and drilling. Essentially, it is a down-hole process consisting of expanding the diameter of the tubular by pushing or pulling a cone through it. Recent extensive research and development work in expandable tubular has provided successful solutions for a variety of difficult problems such as zonal isolation, aged fields, deteriorated casings, difficult-to-access and uneconomical reservoirs, deep drilling, etc. It has also helped to move forward toward the long-desired target of monodiameter wells. Still under development, but has proved its worth to the energy sector, especially due to its economic and environmental benefits. It aims at reducing the incurred and operational cost near 20–30%. These issues are not only long-standing but also have far-reaching consequences in petroleum industry as it involves the industry's most fundamental technologies; wellbore tubular.

Viewed from an engineering mechanics point of view, the tubular expansion is strongly nonlinear due to geometric and material nonlinearities as well as the contact conditions between the tubular and cone. These characteristics pose challenges to obtain viable and accurate solutions. A mathematical model is developed to predict the force required for expansion, variations in length and thickness, surplus deformation, the stress and strain patterns in expanded tubular, and the effect of material velocities in pre and post expansion regions. The governing equations are solved analytically and using finite element method. The use of finite element method is needed to determine the effect of material velocity during expansion. In order to expand the tubular, the required force is determined for various shapes of the mandrel and the cone associated with mandrel shape. The variation in required expansion force also varies with variation in friction coefficients and expansion ratios (ERs). There is an increase in expansion force with an increase in these two parameters. During tubular expansion process, the tubular material above and below the expansion zone gets effected, which was quantified through magnitude of plastic deformation, reduction in tubular wall thickness, and material velocity in pre and post expansion zones. It was found that for lower values of mandrel cone angles and expansion ratios greater than 24%, the tubular fails even at

http://dx.doi.org/10.5772/intechopen.70311

very low friction coefficients. The maximum interfacial stress (contact stress) occurs at 20% expansion ratio while displaying an upward trend with increase in coefficient of friction between the mandrel and the tubular surfaces. Simulation results asserted that the cone, during its progress, defines the new diameter of the tubular and found out that the surplus deformation or the gap between the cone diameter and the expanded tubular inner diameter is negligible. A comparative study is also done between the analytical and simulation results.

2. Literature review

Metal forming operations are classified as processes that are designed to exploit a remarkable property of metal plasticity, the ability to flow as solid without deterioration of properties. The simple rearrangement of the work piece to produce the desired shape and size reduces the waste substantially. To impose such alterations, external forces with appropriate boundary conditions are applied. Tubular expansion, an indirect extrusion method, is an important manufacturing process, which is used in the production of a wide range of products ranging from house hold pipes to boilers and heat exchanger tubes [1, 2]. In recent years, the expansion of circular tubes has drawn more and more attention in much more critical applications where accurate dimensions, smooth surface finishes, and long-term safe and trouble-free operations are of great importance such as catheters for medical application, passive energy absorbers in automotive industry, etc. [3–5].

At the juncture of 20th and 21st centuries, the development of an innovative application of tube expansion in oil and gas industry led to the solid expandable tubular (SET) technology. Multitudes of successful research work was done on concept, significances and applications of solid expandable tubular technology; however, the focus was mostly on industry demand-driven needs. Filippov et al. [6], in his pioneering work, presented three solution scenarios using SET in drilling. First, an expandable open-hole drill liner that can reduce costs and enhance the ability of the operator to access new reservoirs, which are currently difficult to drill economically. Second, expandable cased-hole liner to maintain profitable production from older fields and third is an expandable liner hanger system that can reduce or eliminate the occurrence of the hydraulic leaking of liners, which can improve the economics of drilling deeper and farther.

In SET, the deformation is strongly nonlinear due to large strains, complex material behavior, and contact conditions between the tubular and the mandrel. These characteristics make it quite difficult to obtain exact solution. Decades of research work on cold-work tube forming produced different analytical or semi-analytical models with simplifying assumptions to determine force required to permanently enlarge tube inner diameter, resulting changes in its length and thickness, material strain hardening history, etc. The pioneering work of Hill [7] for tube sinking was a major breakthrough in determining an analytical or semi-analytical solution. However, very limited research work is done on developing analytical and simulation models of tubular expansion process, including inherent nonlinearities, its dynamics, the effect of interaction between the tubular and surrounding fluids, contact mechanics, etc. [8, 9]. Another challenge was accurate prediction of the tubular expansion in irregular shaped boreholes. The

boreholes are mostly not concentric and circular in cross section. This results in oval-shaped expansion of tubular, which does not allow enough clearance for completion tools to pass through. The simulation of such expansion was successfully done using finite element method and design graphs were generated for field engineers to make right decision before lowering the completion to complete an oil well [10]. By combining SET with sidetracking technology, the operators mitigated troublesome shale formations and reached additional reserves with sufficient hole size. In summary, expandable tubular can thus be considered as a potential innovative breakthrough. Although the solid expandable tubular technology provided solutions for many unresolved problems, but limitations remain due to its increased cost, long-term sustainability, and issues related to health, safety and environment. The major obstacle comes from lack of thorough understanding of tubular material and corresponding mechanical strength, once the inner diameter of the tubular is increased beyond 25% of its original value. The prediction of post expansion mechanical properties is necessary to avoid any failure during its service life.

There were very limited attempts that tackled the task of developing a comprehensive analytical model for the tubular expansion process, and mostly under very simplified conditions. For instance, Marciniak and Duncan [11] developed a model for tubular expansion under tension by assuming a constant wall thickness and neglecting the axial strain within the expansion zone. Using a very simplified definition, Stewart et al. [12] considered the tubular expansion process to be similar to a burst test stopped at a pressure between yield pressure and burst rupture pressure. Thus, with aid of the basic definitions of stress and strain along with some empirical equations for burst pressure, very simplified formulations were developed for some of the basic parameters of tubular expansion process like expansion ratio, equivalent plastic strain, burst pressure, and expansion force. The mathematical model developed by Fischer et al. [13] for tube flaring considered the variation in pressure and thickness within the expansion zone and determined the expansion force required to expand thin walled tubes in conical form under compression. Yeh [14] conducted a theoretical study to determine the relationship between punch stroke, tube thickness, expansion ratio, and flaring limit. He found that material strain hardening has no effect on the relationship between thickness variation and expansion ratio. Through relating the assumptions of Marciniak and Duncan [11], Al-Hiddabi et al. [15] used plasticity and membrane theories to develop models for expansion process of thin-walled tubular with a conical expansion tool. The models demonstrated the variation in the force required for expansion with respect to expansion ratio, friction coefficient (μ), mandrel geometry, and tubular material's yield strength. Later, Ruan and Maurer [16] developed another model for tubular expansion process based on force and energy balance principles. This model is capable of estimating the contact pressure at the tubular-mandrel interface, as well as predicting the amount of pressure needed to drive the mandrel forward in order to attain the desired expansion ratio. With an aim of optimizing the mandrel shape, Karrech and Seibi [17] came up with another model for expansion of thin-walled tubular with an aim to estimate stress value, expansion force, and dissipated energy as a result of the expansion process.

First successful attempt to develop a comprehensive analytical model was done by Al-Abri et al. [18], which have reduced significant number of assumptions of previous models. In addition, the results of analytical model fare very well with computational and experimental

http://dx.doi.org/10.5772/intechopen.70311

results in terms of all parameters of interest including the contact pressure between the mandrel and tubular contact zones. For tubulars with threaded connections, a nonuniform contact condition occurs at the mandrel-tubular interface. During expansion of these threaded sections of the tubular, the disengagement of threads results in additional load on adjacent threads, which in turn damages it badly resulting in lowering the dependability of threaded connections [19]. The root cause of such behavior is the axial bending, which can be significantly reduced by lowering the mandrel cone angle from a typical value of 10 to 2°. None of these attempts do properly account for all the effects associated with down-hole expansion process, which demands that the tubular must expand to the desired diameter without fracturing, bursting, or damaging the tubular. At the same time, it must have hydraulic capabilities to provide sufficient resistance against burst and collapse during service. Due to the difficulty in obtaining closed form solutions of the problem in its entirety, researchers opted for approximate solutions using computational methods [20]. The study showed the effects of expansion ratio, friction coefficient, and cone angle on tubular expansion. Even at low values of friction coefficient, the failure could not be avoided for small mandrel cone angles and large expansion ratios. Researchers have tried aluminum tubular due to its improved formability as compared to steel, but the severity of down-hole environment excludes this possibility [21, 22].

In order to analyze the stress, strain, and residual stress induced in the solid expandable tubular applied in repairing casing damaged in wells, Binggui et al. [23] used the commercial finite element method (FEM) package ANSYS to model and simulate the problem. The expansion process induces residual stress in the tubular after expansion. Using the effective measures of the residual stress obtained through the developed model, a proactive action can be taken to reduce the residual stress in tubular through properly designed manufacturing or postprocessing stages. Another important observation drawn from the study was the occurrence of secondary deformation in the SET during the use of high-pressure liquid; it was found that the radius size unilaterally increased by 0.9–1.3 mm. A careful study of published literature shows that most of the developed models for tubular expansion have ignored the dynamic effects by simply assuming that the expansion process occurs out at a very low speed. It is true that under this assumption strain rate effects are negligible but not the dynamic friction conditions, which originates at the interfaces [24].

Right from the inception of SET, a long-term goal has been set for gradually elimination of the conventional telescopic well through the development of slim and monodiameter wells [25–27]. With the help of slim wells, the rate of penetration can be improved, optimal operation of solids control equipment and can achieve lower capacity rigs. Similarly, Matthew [28] defined the challenges and potential of a monodiameter well. The anticipation that expandable monodiameter well will provide the operators an ability to isolate zones that contain reactive shale's, subsalt environments, low fracture gradient formation, or other drilling situations without reducing the casing sizes, is a significant benefit. Due to this, one can reach the reservoir with adequate production hole sections at total depth, hence will avoid adverse effect on oil production. Ruggier et al. [29] have documented the advances in expandable tubing for zonal isolation and casing repair. The main advantage of using expandable tubing as opposed to conventional means is that it can restore the casing to its original integrity without a significant loss in internal diameter. One can also apply SET in fixing the aquifer casing leak

with substantial savings [30]. Carlos et al. [31] and Jennings [32] reported the application of SET in reducing the tapering effect that occurs when using multiple casing strings in deepwater drilling. These expandable systems conserve valuable hole size at total depth. Conserving hole size, or diametric efficiency (DE), allows additional pipe strings to be deployed to drill deeper or farther. Marketz et al. [33] described the application of SET in carbonate reservoirs. The technology, when used on trial basis in more than 20 wells in fractured carbonate reservoirs, demonstrated success with expandable tubular solutions to replace scab liners for fracture shutoff and to replace cement for zonal isolation. In addition, fracture shutoff in the drilling phase with expandable tubular and swelling elastomer has made it possible to reduce water cuts of horizontal wells in a carbonate reservoir.

3. Oil well tubular expansion

The principle behind solid expandable tubular technology in an oil well is simple. The tubular expands by push or pull of the mandrel through the tubular. First, a mandrel is housed in a small section of the tubular and welded to the unexpanded tubular, thus creating a string of expanded and unexpanded sections of the tubular. The mandrel can be pushed forward by using high-pressure fluid at the rear end of the mandrel or can be pulled by using a rod, which is connected to the front end of the mandrel. Either of these moves the mandrel forward resulting in expansion of the tubular. **Figure 1** shows the expanded and unexpanded sections of the tubular along with the mandrel. Due to the forward motion of the mandrel, under application of external force, the tubular deforms from initial inner diameter to the required inner diameter. It is extremely important to maintain the structural integrity of the tubular during the expansion process. The expanded tubular must be able to provide sufficient resistance against burst and collapse during its lifetime operation. Furthermore, critical data such as wall thickness, length changes, postexpansion strength, ductility, burst, and collapse strengths

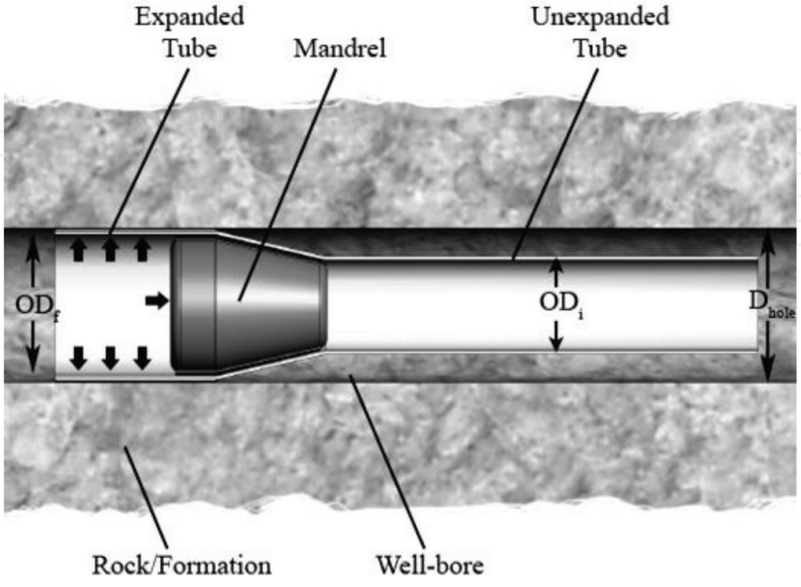


Figure 1. Tubular expansion in an oil well.

http://dx.doi.org/10.5772/intechopen.70311

are essential for its safe and reliable use. During the expansion process, high intensity of stress at the mandrel-tubular interface necessitates careful design of mandrel and selection of its material. In particular, the mandrel geometry becomes important to successfully execute the expansion process.

Ideally, an expanded tubular should have constant diameter and wall thickness over the entire length of the expanded section. Due to the circular cross section of mandrel, it is expected that the expanded tubular cross section will also be circular. Various laboratory and field trials have shown that the expanded sections along the depth remain circular in cross section but their centers may not necessary lie on the same axis. However, if the borehole is of irregular shape, then restricted space for expansion of the tubular results in complex boundary conditions, which result in noncircular cross section of tubular. Expansions in the range of 8–26% of the initial tubular inner diameter have been successfully achieved during full-scale laboratory tests but in field applications, expansions of up to 20% have been successfully attained.

4. Finite element formulation

When studying the deformation of metallic solids due to applied loads, it is common to assume that the material will behave in an isotropic manner. Typically, this assumption is extended to both the elastic and elastic-plastic responses. The forming process may induce anisotropy into the material, giving directionally sensitive elastic-plastic mechanical behavior. Nevertheless, in tube forming (tubular expansion), the induced anisotropy due to permanent deformation is assumed negligible. Huber-Mises yield criterion is used to determine onset of yielding and is updated during the material strain hardening history. Contact between mating surfaces is defined using Coulomb friction law. An associated flow rule, in which the plastic flow potential is assumed to be the yield function, is used to define the elastic-plastic incremental constitutive relation. By means of incremental and iterative procedure, the numerical solution is obtained including expansion force, thickness and length changes, and surplus deformation. The law defining the onset of yielding under combined state is known as the yield criterion. With the assumption of no Bauschinger effect, the final form of yield function, $f(\hat{\sigma})$, as it is required for current analysis is given by

$$f(\hat{\sigma}) = \boldsymbol{\sigma} - S_Y = 0 \tag{1}$$

where $\hat{\sigma}$ is the second order stress tensor, $\boldsymbol{\sigma}$ is the von-Mises or effective stress and S_Y is the yield strength of the tubular material. Using the plastic potential function, $g(\hat{\sigma})$, we can define a flow rule. In the present work, an associated flow rule is assumed, so that the yield and the plastic potential surfaces coincide, i.e., $f = g$. Hence, the plastic flow develops along the normal to the yield surface. The phenomenon whereby yield stress increases with further plastic straining is known as strain hardening. In strain hardening theory of plasticity, one must relate the hardening parameters to the experimental stress-strain curve. A stress variable called effective stress has been defined above. In order to define a corresponding strain variable, called effective plastic strain, which is a function of the plastic strains, the concept of plastic

work, i.e., work conjugate relation, is used. Using simple algebraic manipulation, the final equation for effective plastic strain increment $d\boldsymbol{\varepsilon}_{\mathrm{p}}$, in terms of plastic strain components $d\hat{\varepsilon}_p$ can be written as

$$d\boldsymbol{\varepsilon}_p = \sqrt{(2/3)d\hat{\varepsilon}_p \cdot d\hat{\varepsilon}_p} \tag{2}$$

Once the material yields, its behavior will be partly elastic and partly plastic. During any incremental change of loading, the change in strain is assumed to be decomposed additively into elastic and plastic components, i.e.,

$$d\boldsymbol{\epsilon} = d\boldsymbol{\epsilon}_e + d\boldsymbol{\epsilon}_p \tag{3}$$

The elastic strain increment is related to stress increment through an elastic stress/strain matrix "*D*" [34]. Using the consistency condition, which requires the state of stress to remain on the yield surface during plastic flow, one can derive the following incremental stress/strain relationship:

$$d\hat{\sigma} = \left[D - \left\{D\frac{\partial f}{\partial \hat{\sigma}} * D\frac{\partial f}{\partial \hat{\sigma}}\right\}\left\{E_p + D\frac{\partial f}{\partial \hat{\sigma}} * D\frac{\partial f}{\partial \hat{\sigma}}\right\}^{-1}\right] d\hat{\varepsilon} \tag{4}$$

where the term in brackets represents incremental plastic stiffness matrix [K]. The incremental elastic-plastic stress/strain relation is valid only when there is plastic deformation. Thus before using this relation, we need loading criteria to determine whether the material is in a state of plastic deformation or not. The loading criteria can be obtained using consistency condition, which assures that the stress state remains on the yield surface as given in Eq. (1).

$$\begin{aligned} \frac{\partial f}{\partial \hat{\sigma}} \bullet d\hat{\sigma} \; &> 0: \quad \textit{Loading} \\ \frac{\partial f}{\partial \hat{\sigma}} \bullet d\hat{\sigma} \; &= 0: \quad \textit{Neutral loading} \\ \frac{\partial f}{\partial \hat{\sigma}} \bullet d\hat{\sigma} \; &< 0: \quad \textit{Unloading} \end{aligned} \tag{5}$$

If the material is not in a state of plastic deformation, the elastic stress/strain relation given by Eq. (6) should be used instead of Eq. (4)

$$\mathrm{d}\hat{\sigma} = Dd\hat{\varepsilon} \tag{6}$$

Considering pressure loads "p" and traction forces "t" between surfaces, the incremental principle of virtual work gives:

$$\int_{Volume} \{\delta\varepsilon_i\}^T \{\sigma_i\}\, dV = \int_{Area} p\,\delta u\, dA + \int_{Surface} \delta u\, t\, dS \tag{7}$$

The contact between mandrel and tubular was modeled using Coulomb friction law to account for the induced friction between the interacting surfaces. The general procedure for defining a finite element model from the principle of virtual work is well known and is clearly stated in literature [34]. The final assembled equation for finite element analysis is given below.

$$[K]\{du\} = \{F_{Pressure}\} + \{F_{Contact}\} \tag{8}$$

where [K] and $\{du\}$ are the assembled stiffness matrix and displacements at grid points. Modified Newton-Raphson method is used to obtain the solution. The strain rate effect is neglected in the above formulation due to low mandrel velocity. The rigid body mandrel was set to travel along the axis of the tubular at a low speed of 1.5 m/min to expand the tubular. Due to low mandrel speed, the strain rate effect was assumed to be negligible.

5. Simulation of tubular expansion in vertical well

Finite element method (FEM) is used to simulate both, axisymmetric and 3-dimensional (3-D) models of the expansion process. The finite element formulation described in Section 4 represents a more generalized approach, which is typical in obtaining simulation results using FEM. The formulation can be programmed using a generic computer language but requires extensive effort to get graphical output from simulation results. On the other hand, various commercial finite element programs are available, which use similar approaches and have excellent postprocessing features. Among a host of available commercial software, ABAQUS fits very closely to the above formulation and hence is used for simulation purpose instead of writing own code.

The tubular was modeled as a deformable body with elastic-plastic material behavior; whereas the mandrel was modeled as a rigid body. The mandrel was also constrained from rotation about its own axis. The induced friction between the tubular and mandrel was modeled using Coulomb friction law. The mandrel cone angle was varied from 10 to 45°. Force required for expansion, equivalent plastic strain, effective stress, contact force, thickness and length variations, and surplus deformation were extracted from output data file of simulated cases. **Figure 2(a)** shows the three-dimensional finite element model of the tubular and mandrel. Due to symmetry only one half of the tubular was considered. The tubular was modeled using eight-node brick elements with reduced integration. After trial runs using 2D and 3D models, a 2D axisymmetric model was selected as shown in **Figure 2(b)** due to cost and computational time considerations. The edges of the mandrel were fillet of 6 mm radius to avoid stress concentration. The tubular was held fixed at expanded end and kept free on unexpanded end. This allowed tubular expansion under tension. Expansion ratios of 5–35% were considered for simulation.

ASTM standard test method (ASTM E8) is used to do tests on three tubular specimens. The specimens cut from the tubular material were prepared according the instructions stated in ASTM standard. Tinius Olson universal testing machine is used to conduct tensile test until

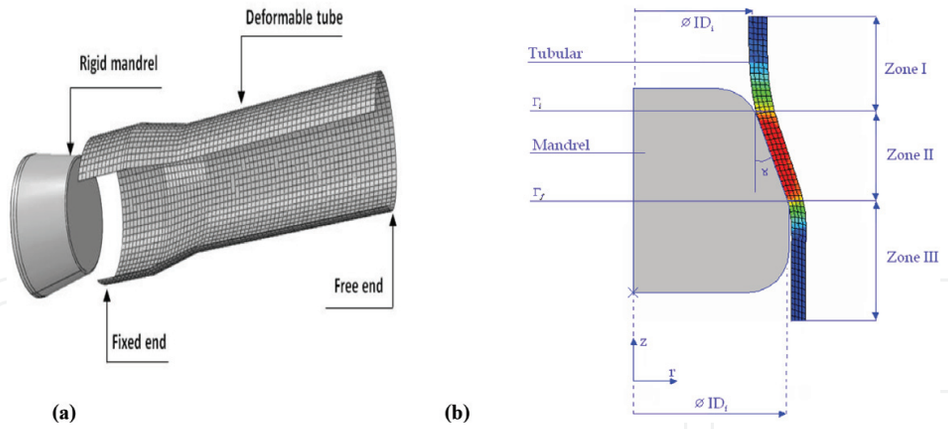


Figure 2. (a) 3-D finite element model; (b) 2-D axisymmetric model with pre- and postexpansion zones.

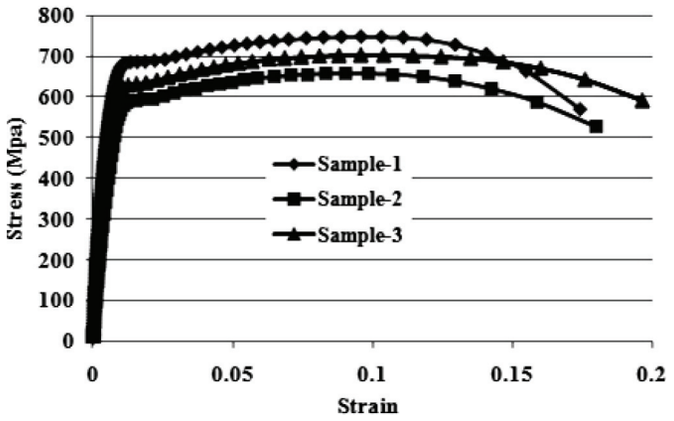


Figure 3. Stress-strain curve for tubular material under uniaxial tensile test.

the specimen fractures. The average of three samples, as shown in **Figure 3**, is then used to determine Young's modulus, yield strength, ultimate tensile strength, strength at fracture, and ductility.

For simulation, the material properties used are the average of these samples. These average stress-strain data are provided as a direct input to the ABAQUS software. The tubular dimensions and other input parameters of finite element model are given in **Table 1**.

Each simulation run consists of two distinct steps. First, it allowed the inner surface of the tubular to expand by prescribing radial displacements up to the final expansion ratio. Then, it released the displacements to establish free equilibrium to define the equilibrium under no load. The stability of the solution is achieved by carefully selecting step sizes. Several factors do affect the solid tubular expansion process; however, the two important parameters for well engineering applications are friction coefficient (μ) and expansion ratio (ER), which were investigated with respect to expansion ratio. Variation in these two parameters will result in an increase in required expansion force. Higher expansion force will lead to two scenarios; (a) need to have larger oil-rig platforms, or (b) need to lower the expansion ratio or friction coefficient, which will reduce the final tubular diameter and hence the target depth of the

Part	Parameters	Value
Tubular (geometry)	Inner diameter	174.625 mm
	Outer diameter	193.675 mm
	Wall thickness	9.525 mm
	Section length	500.000 mm
Tubular (material)	Young modulus of elasticity	210.00 GPa
	Yield strength	615.00 MPa
	Ultimate tensile strength	702.50 MPa
	Poisson's ratio	0.3
	Strain at fracture	0.1966
Mandrel/tubular	Coefficient of friction	0.1/0.2/0.3/0.4
Mandrel	Mandrel cone angle	10°/20°/45°

Table 1. Finite element model input parameters.

reservoirs. The term expansion ratio (ER) is defined as the ratio of difference between the mandrel and the preexpanded tubular diameter to preexpanded tubular diameter.

5.1. Expansion force and stress

Figure 4 shows the stress contours of effective stress for four different expansion ratios at constant values of μ = 0.4 and mandrel cone angle of 20°. Although the stress contours look similar indicating that the expanded zone reaches yielding for all cases, tubular wall thickness decreases with an increasing expansion ratio as discussed in later part of this section. A prior knowledge of expansion requirements is necessary to select appropriate expansion tools and avoid any unexpected failure. The drawing force required for expansion of different tubular sizes is extremely important. Finite element analysis of tubular expansion was carried out to determine expansion force for different expansion ratios, mandrel cone angles and friction at tubular/mandrel interface as shown in **Figures 5** and **6**. **Figure 5** shows the expansion force variation as a function of mandrel position for 25% expansion ratio and different friction coefficients. The maximum force occurs at the beginning of expansion process to overcome inertia, which later drops to almost constant magnitude during rest of the expansion. The small fluctuations in force are due to the transients but overall the expansion process is stable. The average value of expansion force increases to two folds, when μ changes from 0.1 to 0.4. Similar variations in expansion force were found from low expansion ratio (5%) to high expansion ratio (35%) for μ = 0.1 (**Figure 6(a)**). In this case, the increase in average expansion force for 35% ER is more than three time than what is needed for 5% ER. The tubular wall thickness reduces significantly for large expansion ratio and smaller mandrel cone angle. The major part of thickness reduction occurs due to large expansion ratio, which conforms well to volume constancy condition. However, a separate study conducted by authors showed that small cone angle also results in thickness reduction but not to the extent due to large expansion ratios [18]. This phenomenon can be avoided by using a spherical shape mandrel instead of

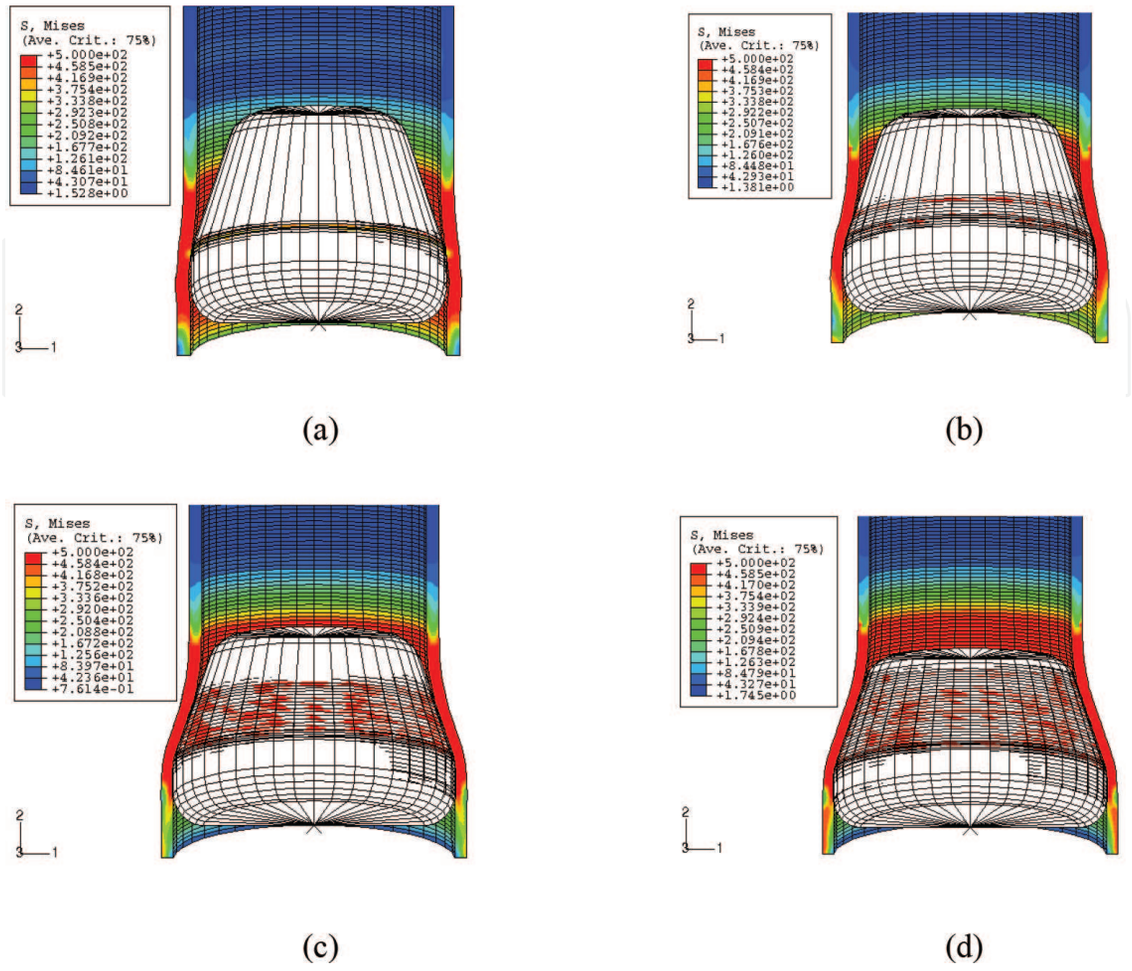


Figure 4. Contours of effective stress, in MPa, for μ = 0.4 and mandrel cone angle of 20°, (a) 5%; (b) 15%; (c) 25% and (d) 35% expansion ratios.

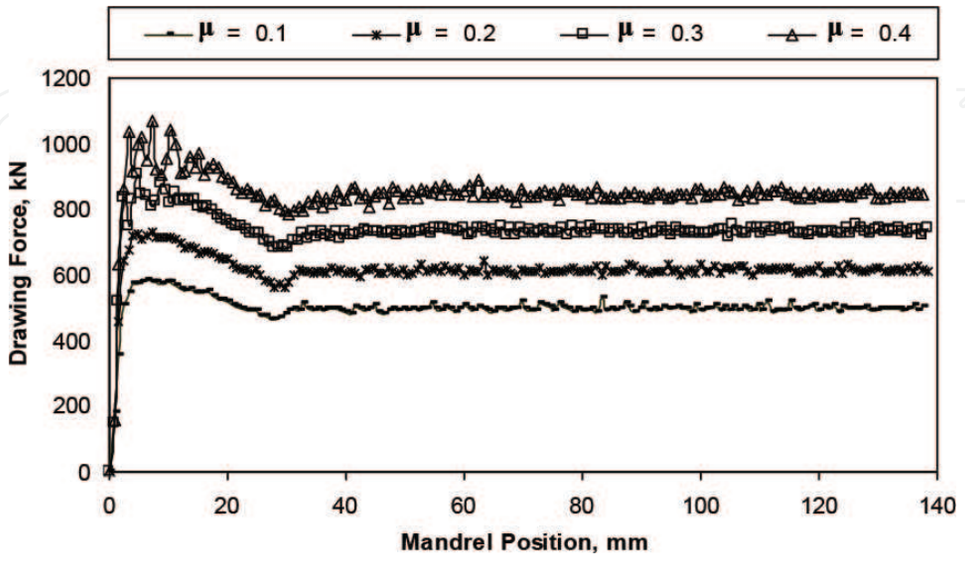


Figure 5. Variation in expansion force w.r.t mandrel position for 25% expansion ratio.

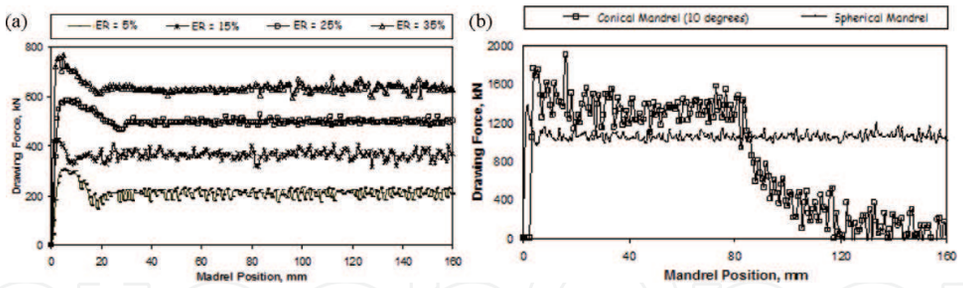


Figure 6. (a) Variation in expansion force w.r.t mandrel position for friction coefficient of 0.1; (b) variation in expansion w.r.t mandrel position for different mandrel shape (μ = 0.4).

conical shape. **Figure 6(b)** shows the variation in expansion force for conical and spherical mandrels for 35% ER and μ = 0.4. The tubular mandrel system remains stable for spherical mandrel and desired expansion is attained successfully. This is true for expansion under tension.

5.2. Material velocity

The velocity variation describes the material flow during the expansion process. To analyze this, divide the tubular into three material zones: I, II, and III as shown in **Figure 2(a)**. Zone I represents the unexpanded section of the tubular, which lies in front of the mandrel. The section of the tubular under expansion is termed as zone II, which is in direct contact with the mandrel. Zone III lies behind the mandrel and represents the expanded section of the tubular. **Figure 7(a) and (b)** show the variation in radial and axial velocity components of the tubular along tubular radius in zones I, II, and III. It is clear from **Figure 7(a)** that there is no change in the radial velocity component, V_r, along the tubular wall thickness, whether it is at zone I or II or III. Contrary to this, the axial velocity component, V_z, remains constant in zone II (z = 237 mm) but varies in other two zones, i.e., in front and back of the mandrel. It decreases in front of the mandrel (z = 217 mm) while increases at the back of the mandrel (z = 257 mm). The reason for this variation is the bending deformation mode of the tubular, which results in alternate tension and compression of inner and outer fibers of the tubular along its wall thickness. To explain it further, the outer and inner fibers of zone I are in compression and tension, respectively. This means that the outer and inner fibers move in the same or opposite direction to the mandrel's motion, which yield higher values of axial velocity in outer fibers as compared to the inner fibers, as shown in **Figure 7**.

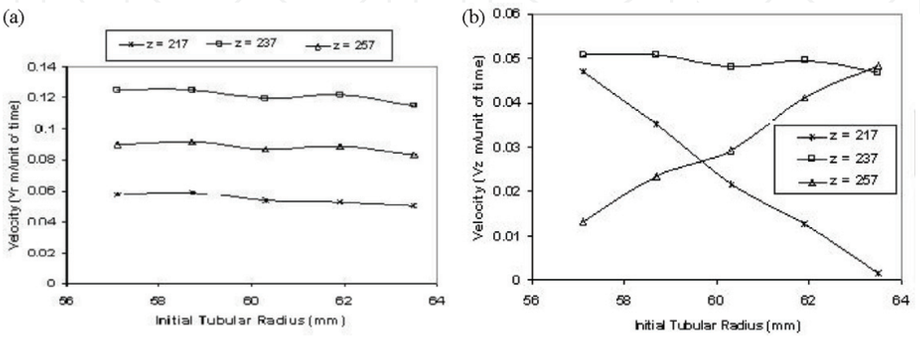


Figure 7. (a) Variation in radial velocity w.r.t tubular radius at different positions along z-axis; (b) variation in axial velocity w.r.t tubular radius at different positions along z-axis.

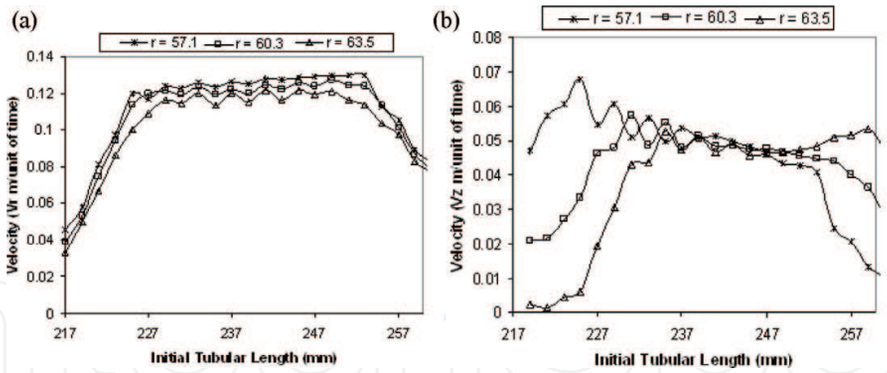


Figure 8. (a) Variation in radial velocity w.r.t tubular axis at different positions along its radius; (b) variation in axial velocity w.r.t tubular axis at different positions along its radius.

The variations in radial and axial velocities along tubular axis at different radial positions are shown in **Figure 8(a) and (b)**. There is an increase in radial and axial velocities with respect to the tubular axis in front of the mandrel, i.e., in zone I and they reduce to zero in the expanded section, i.e., zone III. As we move away from the two ends, only rigid body motion happens between the mandrel and the tubular along the tubular axis. According to the volume constancy, velocities V_z^i and V_z^f (with respect to r) of the surfaces Γ_i and Γ_f, respectively, are related by the following expression:

$$\frac{V_z^f}{V_z^i} = \frac{OD_i^2 - ID_i^2}{OD_f^2 - ID_f^2} \tag{9}$$

Figure 8(b) shows that the velocity in zone II decreases by 20% (0.05–0.04), which is same as predicted by above equation. Therefore, the model accurately predicts material flow along tubular axis. It is worth to mention that the ratio V_z^f/V_z^i decreases with the expansion ratio and increases with the thickness reduction.

5.3. Equivalent plastic strain

The prime reason for tubular expansion is to increase the inner diameter of the tubular. This takes place due to the elastic-plastic deformation of the tubular under applied load. The magnitude of the plastic deformation contributes to the enlargement of the inner diameter and its cumulative effect in terms of strain is termed as equivalent plastic strain. The variation in equivalent plastic strain ε_{eq}^p with respect to radial and axial directions are shown in **Figure 9 (a) and (b)**, respectively. As it can be seen from **Figure 9(a)**, the variation in ε_{eq}^p is negligible along the thickness of the tubular with a maximum in zone III. However, **Figure 9(b)** shows that ε_{eq}^p decreases along the z-direction.

Figures 10(a)–12(b) show the variation in plastic strain components with respect to radial and axial directions satisfying the volume constancy as given below:

$$\dot{\varepsilon}_{rr} + \dot{\varepsilon}_{\theta\theta} + \dot{\varepsilon}_{zz} = 0 \tag{10}$$

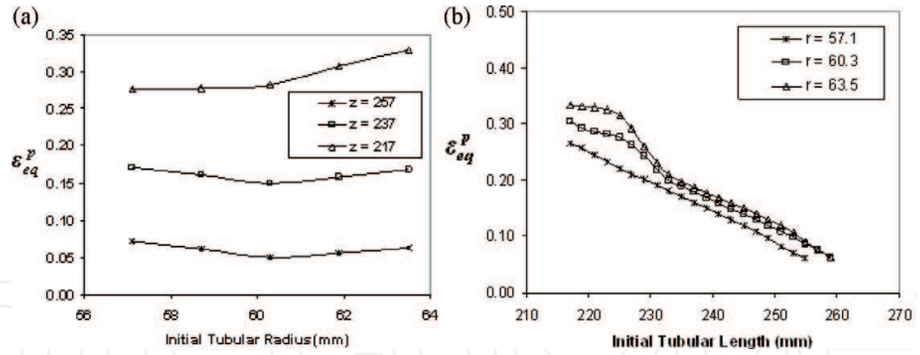


Figure 9. (a) Variation in equivalent plastic strain w.r.t tubular radius at different z-axis values; (b) variation in equivalent plastic strain w.r.t tubular axis at different radial positions.

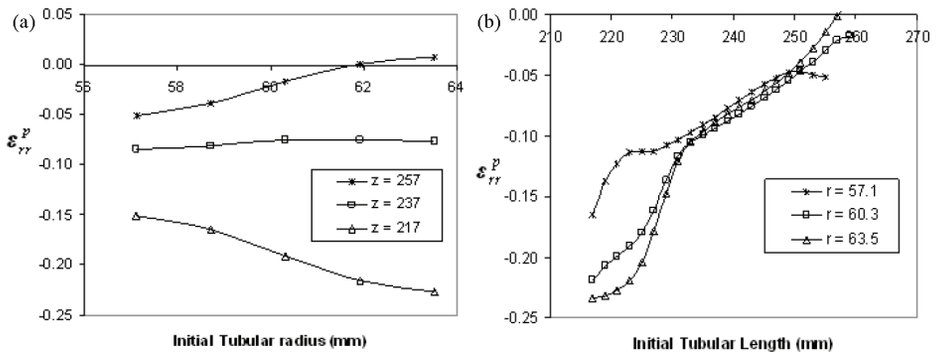


Figure 10. (a) Variation in radial plastic strain w.r.t to tubular radius at different "z" values; (b) variation in radial plastic strain w.r.t tubular axis at different radius.

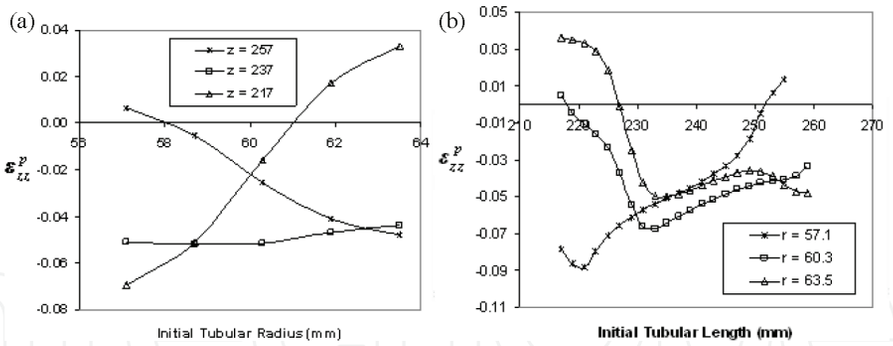


Figure 11. (a) Variation in axial plastic strain w.r.t tubular radius at different positions "z" values; (b) variation in axial plastic strain w.r.t tubular axis at different radius.

Assuming linear rate and neglecting the elastic deformation the components of the plastic strain must satisfy the following equation:

$$\varepsilon_{rr}^{p} + \varepsilon_{\theta\theta}^{p} + \varepsilon_{zz}^{p} = 0 \tag{11}$$

One can verify from **Figures 10(b)**, **11(b)**, and **12(b)** that at any arbitrary point (r = 51.7 mm and z = 257 mm), the components of strain sums to zero, i.e.,

$$\varepsilon_{rr}^{p} + \varepsilon_{zz}^{p} + \varepsilon_{\theta\theta}^{p} = -0.17 - 0.08 + 0.25 = 0 \tag{12}$$

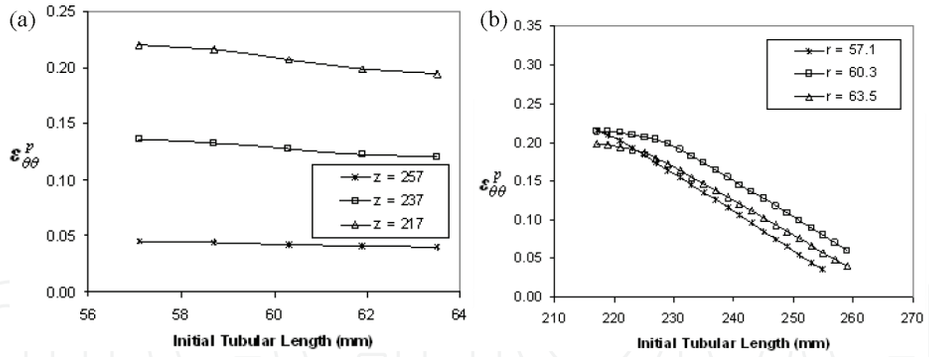


Figure 12. (a) Variation in circumferential plastic strain w.r.t tubular radius at different "z" values; (b) variation in circumferential plastic strain w.r.t tubular axis at different radius.

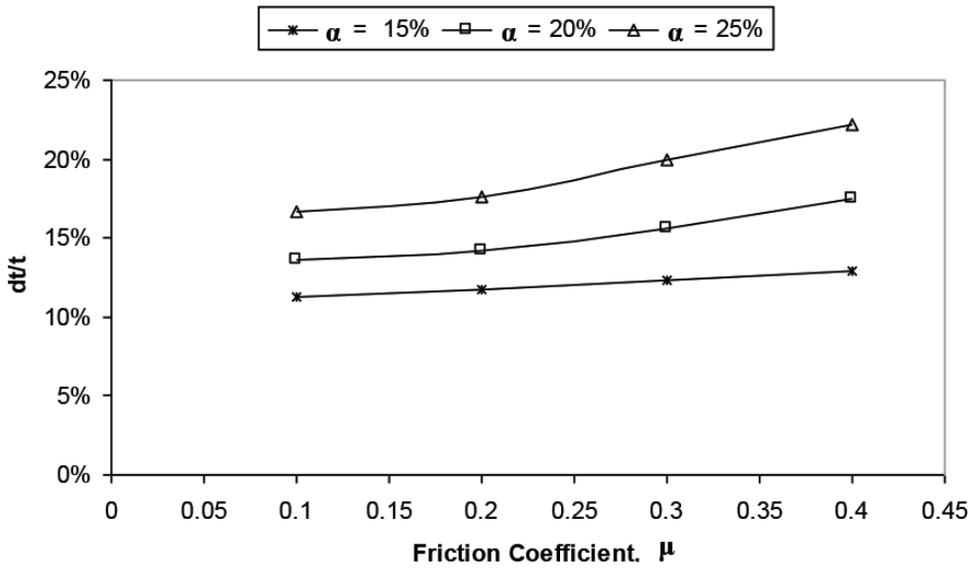


Figure 13. Thickness variation versus coefficient of friction for different expansion ratios.

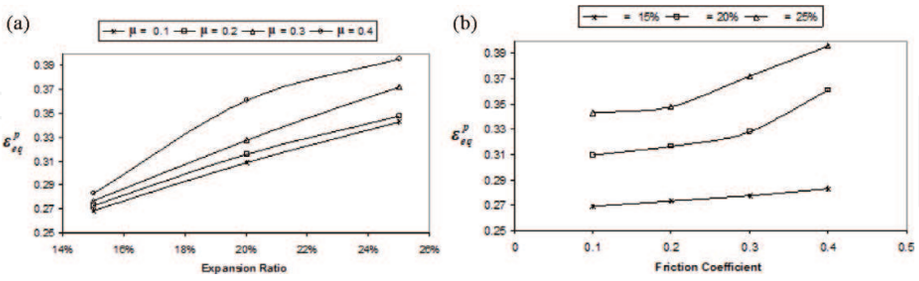


Figure 14. (a) Equivalent plastic strain versus expansion ratios for different friction; (b) equivalent plastic strain versus coefficient of friction for different expansion ratios.

The thickness reduction reached to as high as 25% for an expansion ratio of 25% and friction coefficient of 0.4 as can be seen from **Figure 13**. It also supports the findings of the result shown in **Figure 10(b)**. The reduction in wall thickness of the tubular increases with an increase in coefficient of friction and expansion ratio. This magnitude of reduction will have significant impact on postexpansion strength of the tubular particularly its burst and collapse strengths [18]. **Figure 14(a)** shows that for a fixed value of expansion ratio, the magnitude of

equivalent plastic strain increases with the increase of friction coefficient. However, **Figure 14(b)** shows that for a fixed friction coefficient, the magnitude of equivalent plastic strain increases with expansion ratio. Therefore, it can be concluded that equivalent plastic strain ε_{eq}^{p} increases with friction coefficient and expansion ratio.

5.4. Contact stress

The contact condition between the mandrel and the tubular is of particular interest in tubular expansion. The forward motion of mandrel inside the tubular during expansion results in contact between the inclined surface of mandrel and zone II of the tubular. However, the simulation results show that the contact happens only at small areas at the beginning and end of zone II. The tubular section between the two ends of zone II does not come in contact with the mandrel. To understand this, let's define the normal velocity of the tubular with respect to the mandrel at the mandrel-tubular interface as given below:

$$V_n = V_r \cos\gamma - V_z \sin\gamma \tag{13}$$

where γ is the mandrel angle, which is equal to 20° between the two ends of zone II. However, at the two ends, γ is dependent on fillet radius. If magnitudes of velocities from **Figures 7(a)** to **8(b)** are substituted in above equation, we obtain nonzero velocity V_n in the middle of zone II, which means that there is no contact between the mandrel and the tubular at that particular region. However, full tubular-mandrel contact happens at the front and rear end of the mandrel. From mechanics point of view, it will only be possible, when the material in contact with the mandrel surface at the beginning of zone II is under tension (bottom side) and at the end of zone II is under compression (top side). This represents the bending deformation, which causes the outward deflection along the radial direction. The results of **Figure 15** justifie the presence of gap or no contact between the two ends. The two peaks of stresses are at the two ends of mandrel-tubular interface, while the stress value is zero in between, i.e., in the region of no contact between the tubular and the mandrel.

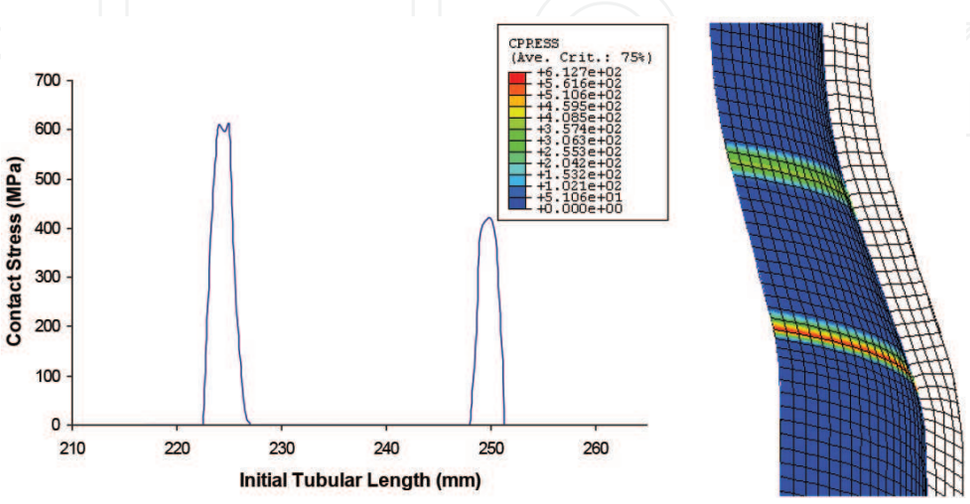


Figure 15. Variation in contact stress, in MPa, at mandrel-tubular interface.

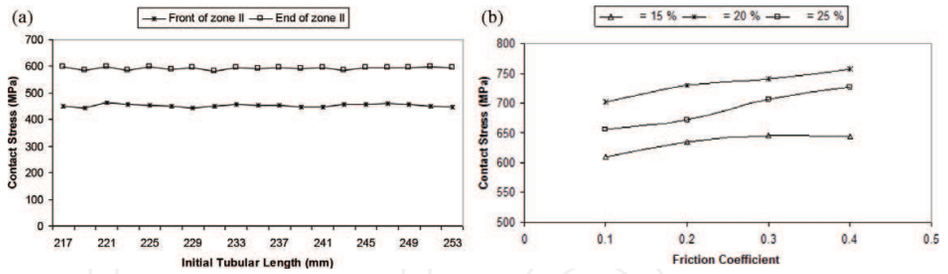


Figure 16. (a) Variation in contact stress, in MPa, at the beginning and end of zone II; (b) back end maximum contact stress versus friction coefficient for different ER.

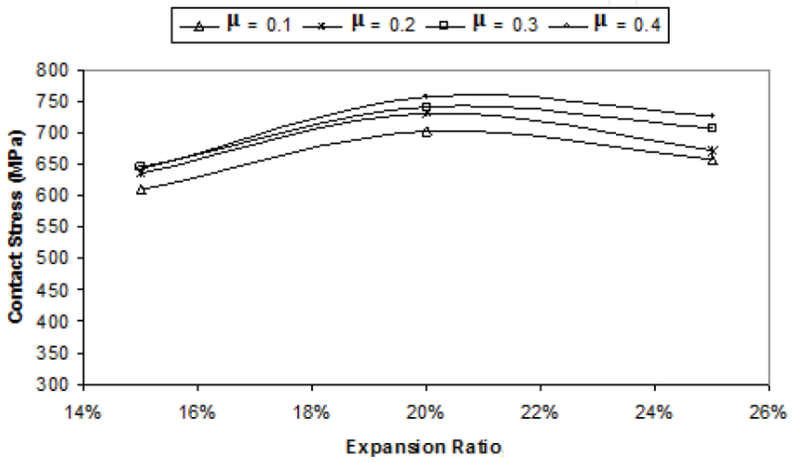


Figure 17. Back end maximum contact stress, in MPa, versus expansion ratio for different μ.

Figure 16(b) shows that for a fixed expansion ratio the maximum contact stress increases with the friction coefficient. However, for a fixed friction coefficient the maximum contact stress occurs at an expansion ratio of 20% as shown in **Figure 17**.

5.5. Effect of friction coefficient

Studying the effects of friction coefficient on expansion force, tubular length and thickness variation as well as the surplus was performed by keeping the mandrel angle and the expansion ratio constant while varying the friction coefficient. This effect was also conducted for various expansion ratios while maintaining the mandrel angle fixed for all cases. Previously published work presented the variation of the drawing force, tubular thickness and length, and surplus variation as a function of the mandrel position, which concluded that the drawing force increases as the friction coefficient increases for all cases regardless of the expansion ratio and the mandrel angle [18]. The force variation peeks at the start-up of the expansion process and decreases to a constant level with small fluctuation as the mandrel advances further indicating that expansion is becoming more stable. It was observed that the tubular thickness reduces as the friction coefficient increases. This reduction keeps increasing to a certain level and stays constant as the mandrel passes the points of interest where the results were extracted. This behavior is the same for all expansion ratios (5–35%) at the mandrel angles of 10 and 20°. However, for a mandrel angle of 45°, the tubular thickness reduction was observed

to increase to a certain level and reduces to show some recovery in the order of 20% of the maximum thinning. The tubular length was observed to shorten and elongates for certain cases. In most of the cases, the tubular length shortens for small values of drawing forces as well as mandrel angles. However, the length elongates for higher drawing forces causing the expanded section to elongate further due to tension. Therefore, it can be concluded that the variation in tubular length depends heavily on the magnitude of the drawing force, which in turns depends on the tubular expansion, resistive force due to friction between metal surfaces, mandrel cone angle, and bending.

5.6. Effect of expansion ratio

Similar observations to the drag effect were made when studying the effect of expansion ratio on expansion force, tubular length and thickness, and tubular surplus while maintaining the other parameters constant. It was found that the expansion force and tubular surplus increase while the tubular thickness keeps thinning as the expansion ratio increases ratio irrespective to the mandrel angle and the friction coefficient. However, the tubular length variation shows similar behavior as that of the drag effect. It is important to note that the surplus deformation depends on the hardening behavior of tubular material. The difference in tubular final and desired inner diameters in terms of desired inner diameter is called surplus deformation. As a result of tubular expansion, the final tubular inner diameter will not be the exact required value. This happens due to the material's elastic recovery once the mandrel passes the expansion zone and the system dynamics of coupled system under consideration. The elastic recovery will be more in materials with lower hardening coefficient and hence influence the surplus deformation. This means that the hardening behavior of tubular material will have an effect on the magnitude of surplus deformation.

6. Anticipated failures and envisaged solutions

Occasionally, some of the mandrel geometric configurations combined with the irregular mandrel/tubular interaction as well large expansion ration may cause tubular failure. When a mandrel angle is 10°, the surface contact area is maximum between the mandrel and the tubular. If in such case the friction coefficient is high ($\mu = 0.4$) and expansion ratio approaches 35%, simulation results showed that the tubular will fail due to excessive wall thinning ultimately leading to rupture. Similar behaviors are also observed under other severe conditions. **Figure 18** shows two cases where the tubular has failed due to large magnitudes of expansion force, which subjects the tubular to extreme tension in post expansion zone. In order to avoid such failures, three solutions are proposed:

(a) Expand the tubular under compression instead of tension for the same mandrel angle, 10 and 20° (fix the top part of the tubular while running the mandrel from bottom upwards).

(b) Expand the tubular under plane strain condition for the same mandrel angle, 10 and 20° (fix the top and bottom parts of the tubular while running the mandrel bottom upwards).

(c) Use a spherical mandrel, if desire is for bottom-up tubular expansion under tension.

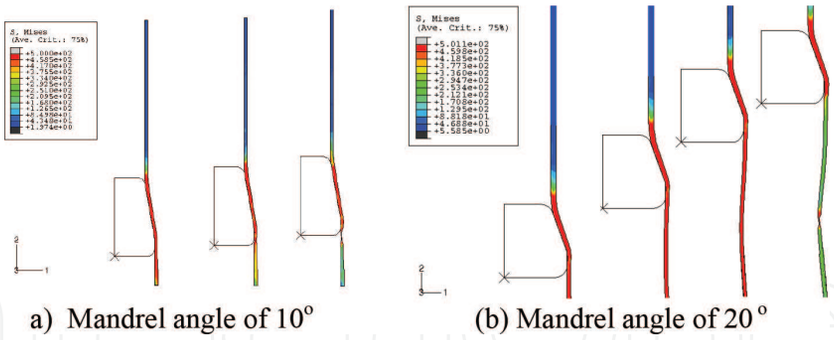


Figure 18. Simulation results showing tubular failure for $\mu = 0.4$ and 35% expansion ratio.

7. Rotating mandrel

Simulations have also been carried out to investigate the effect of the mandrel rotation on estimated drawing force required for expansion, surplus deformation, and thickness and length variations as shown in **Figure 19**. The results are obtained for 20° mandrel cone angle, 15% expansion ratio, μ = 0.1 and 5 mm thick seal wrapped around the tubular. As can be observed from **Figure 19(a)**, the drawing force required for expansion decreases considerably due to the rotating mandrel. This could be due to the screw effect of the rotating mandrel. However, one must keep in mind that proper lubrication and additional power is needed to rotate the mandrel. The lesser magnitude of extrusion force for a rotating mandrel can be

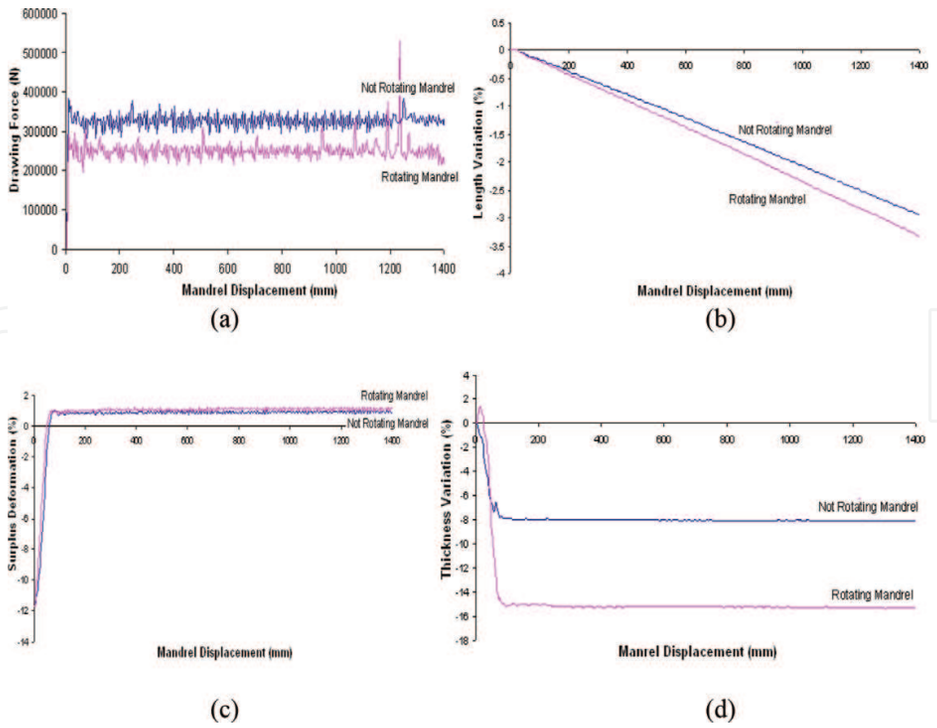


Figure 19. Plot of (a) drawing force, (b) length variation, (c) surplus deformation, (d) thickness variation versus mandrel displacement along the tubular for rotating and not rotating mandrel.

counter balanced by the extra power required for rotation. One has to estimate the total power requirement for the system to have a justifiable comparison between the rotating and nonrotating mandrel. Contrary to this, the thickness variation for rotating mandrel is approximately 47% higher than that of nonrotating mandrel (**Figure 19(d)**). A similar observation, but of lesser magnitude, is observed for length variation (**Figure 19(b)**). There is negligible effect on surplus expansion (**Figure 19(c)**). As pointed out earlier, higher magnitudes of variations in length and especially in thickness may cause structural instability in expanded tubular during its operational life.

Author details

Tasneem Pervez*, Sayyad Z. Qamar, Omar S.A. Al-Abri and Rashid Khan

*Address all correspondence to: tasneem@squ.edu.om

Mechanical and Industrial Engineering Department, College of Engineering, Sultan Qaboos University, Oman

References

[1] Koc M, Altan T. Prediction of forming limits and parameters in the tube hydroforming process. International Journal of Machine Tools & Manufacture. 2002;**42**:123-138

[2] Almeida BPP, Alves ML, Rosa PAR, Brito AG, Martins PAF. Expansion and reduction of thin-walled tubes using a die: Experimental and theoretical investigation. International Journal of Machine Tools & Manufacture. 2006;**46**:1643-1652

[3] Palengat M, Chagnon G, Favier D, Louche H, Linardon C, Plaideau C. Cold drawing of 316L stainless steel thin-walled tubes: Experiments and finite element analysis. International Journal of Mechanical Sciences. 2013;**70**:69-78. DOI: 10.1016/j.ijmecsci.2013.02.003

[4] Yang J, Luo M, Hua Y, Lu G. Energy absorption of expansion tubes using a conical–cylindrical die: Experiments and numerical simulation. International Journal of Mechanical Sciences. 2010;**52**(5):716-725. DOI: 10.1016/j.ijmecsci.2009.11.015

[5] Yan J, Yao S, Xu P, Peng Y, Shao H, Zhao S. Theoretical prediction and numerical studies of expanding circular tubes as energy absorbers. International Journal of Mechanical Sciences. 2016;**105**:206-214. DOI: 10.1016/j.ijmecsci.2015.11.022

[6] Filippov A, Mack R, Cook L, York P, Ring L, McCoy T. Expandable tubular solutions. In: SPE Annual Technical Conference; 3-6 October 1999; Houston, Texas; SPE 56500

[7] Hill R. The Mathematical Theory of Plasticity. New York: Oxford University Press; 1970

[8] Pervez T, Seibi AC, Karrech A. Simulation of solid tubular expansion in well drilling using FEM. Journal of Petroleum Science and Technology. 2005;**23**:775-794

[9] Pervez T, Seibi AC, Karrech A. Analytical solution for wave propagation due to pop-out phenomenon in solid expandable tubular system. Journal of Petroleum Science and Technology. 2006;**24**(8):923-942

[10] Pervez T, Qamar SZ, Al-Hiddabi SA, Al-Jahwari FK, Marketz F, Al-Houqani S, Velden M. Tubular expansion in irregularly shaped boreholes: Computer simulation and field measurement. Petroleum Science & Technology. 2011;**29**:735-744

[11] Marciniak Z, Duncan JL. Mechanics of Sheet Metal Forming. New York: Edward Arnold; 1992

[12] Stewart RB, Marketz F, Lohbeck WCM, Fischer FD, Daves W, Rammerstorfer FG, Böhm HJ. Expandable wellbore tubular. In: SPE Technical Symposium; 16 October 1999; Dhahran, Saudi Arabia; SPE-60766

[13] Fischer FD, Rammerstorfer FG, Daxner T. Flaring—An analytical approach. International Journal of Mechanical Sciences. 2006;**48**:1246-1255

[14] Yeh FH. Study of flaring forming limit in the tube flaring process. Journal of Strain Analysis. 2007;**42**(5):315-342

[15] Al-Hiddabi SA, Seibi AC, Pervez T. Stress analysis of casings expansion/post-expansion: Theoretical approach. In: ASME 6th Biennial Conference Engineering Systems Design and Analysis (ESDA2002/APM-92); 8-12 July 2002; Istanbul, Turkey

[16] Ruan CG, Maurer WC. Analytical model for casing expansion. In: SPE/IADC Drilling Conference; 23-25 February 2005; Amsterdam, Netherlands; SPE-92281

[17] Karrech A, Seibi A. Analytical model for the expansion of tubes under tension. Journal of Materials Processing Technology. 2010;**210**(2):356-362. DOI: 10.1016/j.jmatprotec.2009.09.024

[18] Al-Abri OS, Pervez T. Structural behavior of solid expandable tubular undergoes radial expansion process: Analytical, numerical and experimental approaches. International Journal of Solids and Structure. 2013;**50**(19):2980-2994

[19] DeLange R, Gandikota R, Osburn S. A major advancement in expandable connections performance, enabling reliable gastight expandable connections. SPE Drilling & Completion. 2011;**26**(3):412-418. DOI: 10.2118/135462-PA

[20] Seibi AC, Al-Hiddabi SA, Pervez T. Structural behavior of solid tubular expansion under large plastic deformation. ASME Journal of Energy Resources & Technology. 2005;**127**(4):323-326

[21] Gelfgat MY, Basovich VS, Tikhonov VS. Drill string with aluminum pipes designs and practices. In: SPE/IADC Drilling Conference; 19-21 February 2003; Netherlands; SPE-79873

[22] Pervez T, Qamar SZ, Seibi AC, Al-Jahwari FK. Use of SET in cased and open holes: Comparison between aluminum and steel. Journal of Materials and Design. 2008;**29**(4):811-817

[23] Binggui X, Yanping Z, Hui W, Hongwei Y, Tao J. Application of numerical simulation in the solid expandable tubular repair for casing damaged wells. Petroleum Exploration and Development. 2009;**36**(5):651-657

[24] Al-Abri OS, Pervez T, Al-Hidaabi SA, Qamar SZ. Analytical model for stick-slip phenomenon in solid tubular expansion. Journal of Petroleum Science and Engineering. 2015;**125**: 218-233

[25] Owoeye O, Aihevba LO, , Hartmann RA, Ogoke VC. Optimization of well economics by application of expandable tubular technology. In: IADC/SPE Drilling Conference; 23-25 February 2000; New Orleans, Louisiana; SPE-59142-MS

[26] Gusevik R, Merritt R. Reaching deep reservoir targets using solid expandable tubulars. In: SPE Annual Conference and Exhibition; 29 September-2 October 2002; San Antonio, Texas; SPE 77612

[27] Tubbs D, Wallace J. Slimming the wellbore design enhances drilling economics in field development. In: SPE Annual Technical Conference and Exhibition; 24-27 September 2006; San Antonio, Texas; SPE 102929

[28] Matthew J. World's first expandable monobore well system: Development, implementation and significance. In: International Petroleum Technology Conference (IPTC); 4-6 December 2007; IPTC-11587

[29] Ruggier M, Scott B, Urselman R, Mossor H, Van Noort RHJ. Advances in expandable tubing – A case history. In: SPE/IADC Drilling Conference; 27 February-1 March 2001; Netherlands; SPE-67768

[30] Bargawi RA, Zhou S, Al-Umran MI, Aghnim W. Expandable tubular successfully scab off severe casing leaks. In: SPE/IADC Middle East Drilling Technology Conference and Exhibition; 12-14 September; Dubai, UAE; SPE-97357

[31] Carlos E, Dean B, Waddell K. Increasing solid expandable tubular technology reliability in a myriad of down-hole environment. In: SPE Latin American and Caribbean Petroleum Engineering Conference;27-30 April 2003; Port-of-Spain, Trinidad and Tobago; SPE-81094

[32] Jennings L. Dynamic formations rendered less problematic with solid expandable tubular. In: IADC/SPE Drilling Technology Conference and Exhibition; 25-27 August 2008; Jakarta, Indonesia; SPE-114678

[33] Marketz F, Welling RWF, Noort RV, Baaijens TN. Expandable tubular completions for carbonate reservoirs. SPE Drilling & Completion. 2007;**22**(1):01-07. DOI: 10.2118/88736-PA

[34] Bathe KJ. Finite Element Procedures in Engineering. New Jersey: Prentice Hall; 2007

IntechOpen

IntechOpen